Vietnam Journal of Mechanics, Vol. 44, No. 3 (2022), pp. 266 – 279
DOI: https://doi.org/10.15625/0866-7136/17331

CONCURRENT MULTISCALE TOPOLOGY OPTIMIZATION: A HYBRID APPROACH

Minh Ngoc Nguyen[1,*], **Tinh Quoc Bui**[1]
[1]*Duy Tan Research Institute for Computational Engineering (DTRICE) - Duy Tan University, 06 Tran Nhat Duat street, District 1, Ho Chi Minh City, Vietnam*
[*]E-mail: nguyenngocminh6@duytan.edu.vn

Received: 20 July 2022 / Published online: 10 September 2022

Abstract. This paper presents a hybrid approach for multiscale topology optimization of structures. The topological shape of both macro-structure and micro-structure are concurrently optimized, based on the solid isotropic material with penalization (SIMP) technique in combination with finite element method (FEM). The material is assumed to have periodically patterned micro-structures, such that the effective properties can be evaluated via energy-based homogenization method (EBHM). In every iteration, the effective properties of material are passed to the macroscopic problem, and the macroscopic behavior (e.g. strain energy) is transferred back to the micro-scale problem, where the unit cell representing the micro-structure of material is determined for the next iteration. It is found that the update process can be done separately, i.e., the sensitivity of macro-scale design variables is not required during the update of micro-scale design variables, and vice versa. Hence, the proposal is that the macro-structure is updated by the gradient-free Proportional Topology Optimization (PTO) algorithm to utilize the computational efficiency of PTO. The micro-structure is still updated by the common gradient-based algorithm, namely Optimality Criteria (OC). Three benchmark numerical examples are investigated, demonstrating the feasibility and efficiency of the proposed hybrid approach.

Keywords: concurrent topology optimization, hybrid, energy-based homogenization method, gradient-free, PTO algorithm.

1. INTRODUCTION

Since the pioneering work by Bendsøe and Kikuchi [1], topology optimization has been attracting much attention from both the academic and industrial communities. In short, the target is to obtain a material layout that maximizes a specified performance of a structure, under certain constraints and given loading and boundary conditions. Early, the layout is simply described by a discrete field of (pseudo) density that takes values of 0 or 1 to represent whether an element is voided or completely filled by material [1]. In order to overcome the numerical issues caused by the discrete description, the (pseudo) density is then expressed as a continuous field varying from 0 to 1 [2, 3]. Together with

that, the Solid Isotropic Material Penalization (SIMP) method is introduced, in which a power-law scheme is applied to interpolate the material properties with respect to the density value. Furthermore, the intermediate densities would be penalized to tend to 0 or 1 during the optimization process. Alternatively, a rational scheme, namely the Rational Approximation of Material Properties (RAMP) [4] can be used. Instead of density-based approaches, there exist other methods such as the level set method [5, 6] and the phase field method [7, 8], where the equation for evolution of level set or phase field is solved to get the representation of material layout.

Sensitivity analysis, i.e., the derivative of the objective function and the constraint with respect to design variables, is usually required. On the contrary, a gradient-free approach updates the design variables without sensitivity information. However, the early gradient-free attempts that use meta-heuristic search in combination with a discrete field of pseudo density (0 or 1) has been criticized for inefficiency [9]. Recently, the Proportional Topology Optimization (PTO) algorithm has been introduced by Biyikli and To [10] for the problem of compliance minimization. The idea behind PTO is simple: material is distributed to each element, proportionally to the contribution of that element in the total compliance (a measure of elastic strain energy). The PTO method has been later further extended for multi-material problems [11] and design of Reissner-Mindlin plates [12], demonstrating its competitiveness. An improved version of PTO was proposed by Ref. [13]. A high-resolution yet efficient approach is also achieved by combining PTO and meshfree analysis, as reported in Ref. [14]. Besides PTO, there exist some other interesting gradient-free algorithms such as the cellular automata [15], the derivative-free level set method [16], and the Kriging-based material field series expansion [17]. Indeed, compared to the majority of gradient-based approaches, the number of works on gradient-free topology optimization is still very limited. Hence, further exploration on this area is needed.

Recently, attraction has been paid for concurrent topology optimization of both material and structure. In short, this is a two-scale approach, in which the structural layout (macroscopic level) is determined simultaneously with the material micro-structure, see e.g. [18–21]. The assumption would include linear elastic behavior and the periodic repetition of micro-structure within the macro-level structure. Homogenization scheme is employed to evaluate the effective material property. An instruction on numerical implementation of homogenization could be found in [22]. The concept of two-scale topology optimization has been so far employed in various types of problems, for e.g., design of elastic structures [18–20], heat-conductive structures [23, 24], thermo-elastic structures [25, 26], etc. When the orientation of micro-structure and/or the existence of multiple types of micro-structures are taken into account [21, 27, 28], attention should be paid for the connectivity between the micro-structures [29, 30]. Designs of porous lattice structures without material homogenization in the micro-structure were also introduced, based on the adaptive geometric components [31–33]. However, the development so far generally relies on gradient-based methods. To the best knowledge of the authors, attempts on application of gradient-free algorithm into multi-scale topology optimization have not been discussed in the available literatures.

In this paper, a hybrid approach for density-based concurrent topology optimization of multi-scale structures is proposed. A well-known gradient-based optimizer, namely Optimality Criteria (OC) is utilized for the update of micro design variables. For macro-scale problem, the gradient-free Proportional Topology Optization algorithm is employed, in order to gain the computational efficiency.

The rest of the paper is organized as follows. Right after the Introduction is the formulation of the hybrid approach for multi-scale topology optimization in Section 2. Three numerical examples are presented and discussed in Section 3 to demonstrate the feasibility of the proposed approach. Finally, some concluding remarks are given in Section 4.

2. FORMULATION OF THE TWO-SCALE TOPOLOGY OPTIMIZATION

2.1. Mathematical description of the problem

The multi-scale problem being considered is sketched in Fig. 1. The goal is minimization of the structural compliance (i.e., a measure of elastic strain energy of the macro-structure), see Eq. (2), together with determination of the micro-structure. The micro-structure is assumed to be periodically repeated within the macro-structure. Thus, a representative unit cell can be considered and effective material properties can be evaluated using homogenization technique. Mathematically, the multi-scale optimization problem is stated as follows

$$\text{Find}: \ \rho_i \in [0,1], \ \rho_{m,j} \in [0,1], \ (i = 1,2,3,\ldots,N), \ (j = 1,2,3,\ldots,N_m) \tag{1}$$

$$\text{Objective}: \text{minimize } c = \int_{\Omega} \left(\boldsymbol{\varepsilon}\left(\mathbf{u}\right)\right)^T \mathbf{D}\boldsymbol{\varepsilon}\left(\mathbf{u}\right) \mathrm{d}\Omega = \mathbf{u}^T\mathbf{K}\mathbf{u}, \tag{2}$$

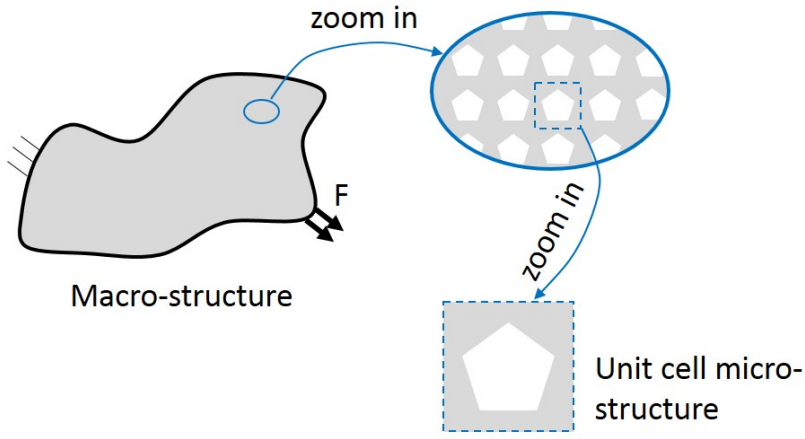

Fig. 1. Schematic sketch of model for design of multi-scale structures

subject to

$$\mathbf{K}\mathbf{u} = \mathbf{F}, \tag{3}$$

$$\int_{\Omega^m} \left(\boldsymbol{\varepsilon}\left(\delta\mathbf{u}_m\right)\right)^T \mathbf{D}_m \boldsymbol{\varepsilon}\left(\mathbf{u}_m\right) \mathrm{d}\Omega_m = \int_{\Omega^m} \left(\boldsymbol{\varepsilon}\left(\delta\mathbf{u}_m\right)\right)^T \mathbf{D}_m \boldsymbol{\varepsilon}\left(\mathbf{u}_m^0\right) \mathrm{d}\Omega_m, \tag{4}$$

$$\int_{\Omega} \rho \mathrm{d}\Omega = \sum_i \rho_i V_i \leq \bar{v}|\Omega|, \tag{5}$$

$$\int_{\Omega_m} \rho_m \mathrm{d}\Omega_m = \sum_i \rho_{m,i} V_{m,i} \leq \bar{v}_m |\Omega_m|. \tag{6}$$

Here, quantities in micro-scale are denoted with subscript "m", while those in macro-scale are denoted without subscript. c is the structural compliance, which should be minimized in the optimization process. The design variables, ρ and ρ_m, are pseudo densities for macro-scale and micro-scale problems, respectively, which are defined as element-wise constants in finite element analysis. The number of variables, N and N_m, are thus associated with the number of elements being used for discretization of the two domains, which in turn are denoted by Ω and Ω_m. In Eq. (2), $\boldsymbol{\varepsilon}$ contains the strain components, which are computed from displacements. The "mass constraints" in the two scales are provided in Eq. (5) and Eq. (6), in which V_i and $V_{m,i}$ are the "volume" of an arbitrary element i (for two-dimensional domain, it is the element area) in macro- and micro-domains, respectively. $\bar{v}$ and $\bar{v}_m$ are the required volume fractions. $\mathbf{u}$, $\mathbf{K}$, and $\mathbf{F}$ in Eq. (3), which describes equilibrium of macro-structure, are respectively the vector of nodal displacement, the stiffness matrix and the load vector. Vector $\delta\mathbf{u}$ consist of the virtual displacements. Eq. (4) is the equilibrium equation in the representative unit cell, arising from the energy-based homogenization method (EBHM), which is presented in the following section.

2.2. Energy-based homogenization method

The effective macroscopic property of the material is numerically evaluated using the energy-based homogenization method (EBHM) [20, 34], providing the link between macro- and micro-scale problems. Within the scope of linear elasticity, homogenization method can be applied to estimate the macroscopic effective properties of materials [35]. For higher accuracy in estimation, two further assumptions need to be fulfilled: (1) the size of micro-structure must be much smaller than that of the bulk sample, and (2) the micro-structure is distributed periodically within the macro-structure [20, 34]. Assuming that the micro-structure is given in a unit cell $\Omega_m = \left[0, x^0\right] \times \left[0, y^0\right]$, the homogenized elastic tensor can be written using the EBHM as follows [20, 34]

$$\mathbf{D}^H = \frac{1}{|\Omega_m|} \int_{\Omega^m} \left(\boldsymbol{\varepsilon}\left(\mathbf{u}_m^0\right) - \boldsymbol{\varepsilon}\left(\mathbf{u}_m\right)\right)^T \mathbf{D}_m \left(\boldsymbol{\varepsilon}\left(\mathbf{u}_m^0\right) - \boldsymbol{\varepsilon}\left(\mathbf{u}_m\right)\right) \mathrm{d}\Omega_m, \tag{7}$$

where $\mathbf{D}_m$ is the locally varying elastic tensor and $\boldsymbol{\varepsilon}_m^0$ is the linearly independent unit test strain field. The strain field within the micro-structure, $\boldsymbol{\varepsilon}_m$, is the solution of the equilibrium equation with periodic boundary condition given in Eq. (4). The tensor $\mathbf{D}_m$ is computed at each element (of the micro domain) using the Solid Isotropic Material

with Penalization (SIMP) technique (see e.g. [36]) as

$$\mathbf{D}_m(\rho_{m,j}) = \left(k + (1-k)\rho_{m,j}^p\right)\mathbf{D}_0, \tag{8}$$

where $\mathbf{D}_0$ is the elastic tensor of the base material. Here k is a small positive number to avoid zero stiffness when $\rho_{m,j}$ tends to 0. Parameter p is the exponent factor which helps to penalize the intermediate densities during optimization process. In this paper, $p = 3$ is chosen.

2.3. Sensitivity analysis with respect to micro-scale design variables

The (macro-scale) global stiffness matrix $\mathbf{K}$ in Eq. (2) is assembled from the element stiffness matrix as follows

$$\mathbf{K} = \int_\Omega \left(\boldsymbol{\varepsilon}\left(\delta\mathbf{u}\right)\right)^T \mathbf{D}\boldsymbol{\varepsilon}\left(\mathbf{u}\right)\mathrm{d}\Omega = \sum_{i=1}^{N}\mathbf{K}_{e,i}, \tag{9}$$

where N is the number of elements and the stiffness matrix of element i, $\mathbf{K}_{e,i}$, is given by

$$\mathbf{K}_{e,i} = \int_{\Omega^{e,i}} \left(\boldsymbol{\varepsilon}\left(\delta\mathbf{u}\right)\right)^T \mathbf{D}(\rho_i)\left(\boldsymbol{\varepsilon}\left(\mathbf{u}\right)\right)\mathrm{d}\Omega, \tag{10}$$

in which $\boldsymbol{\varepsilon}$ is the strain tensor and $\mathbf{D}(\rho_i)$ is the elastic tensor with respect to the (pseudo) density. Applying the SIMP technique, $\mathbf{D}(\rho_i)$ is calculated as

$$\mathbf{D}(\rho_i) = \left(k + (1-k)\rho_i^p\right)\mathbf{D}^H, \tag{11}$$

where $\mathbf{D}^H$ is the homogenized elastic tensor of the base material (see Eq. (7)).

Sensitivity analysis with respect to micro design variable $\rho_{m,j}$ gives [20]

$$\frac{\partial c}{\partial \rho_{m,j}} = -\mathbf{u}^T\frac{\partial \mathbf{K}}{\partial \rho_{m,j}}\mathbf{u} = -\int_\Omega \left(\boldsymbol{\varepsilon}\left(\mathbf{u}\right)\right)^T\frac{\partial \mathbf{D}}{\partial \rho_{m,j}}\boldsymbol{\varepsilon}\left(\mathbf{u}\right)\mathrm{d}\Omega \tag{12}$$

in which

$$\frac{\partial \mathbf{D}}{\partial \rho_{m,j}} = \left(k + (1-k)\rho_i^p\right)\frac{\partial \mathbf{D}^H}{\partial \rho_{m,j}}. \tag{13}$$

From Eq. (7), we have

$$\frac{\partial \mathbf{D}^H}{\partial \rho_{m,j}} = \frac{1}{|\Omega_m|}\int_{\Omega^m}\left(\boldsymbol{\varepsilon}\left(\mathbf{u}_m^0\right) - \boldsymbol{\varepsilon}\left(\mathbf{u}_m\right)\right)^T\frac{\partial \mathbf{D}_m}{\partial \rho_{m,j}}\left(\boldsymbol{\varepsilon}\left(\mathbf{u}_m^0\right) - \boldsymbol{\varepsilon}\left(\mathbf{u}_m\right)\right)\mathrm{d}\Omega_m. \tag{14}$$

Using Eq. (8), the derivative of tensor $\mathbf{D}_m$ with respect to $\rho_{m,j}$ is computed by

$$\frac{\partial \mathbf{D}_m}{\partial \rho_{m,j}} = p\left(1-k\right)\rho_{m,j}^{p-1}\mathbf{D}_0. \tag{15}$$

The sensitivity in Eq. (12) is an integral being evaluated in the macro domain. And sensitivity has to be calculated for every micro-scale design variable. This process could be costly in terms of computer memory and computational time. The Matlab code given in Ref. [20] is highly effective when elements (of both domains) take the shape of a square

with unit length. However, for more general cases, when design domains with more complicated shape are involved, an efficient procedure is required. It is noted that Eq. (12) has the same form with Eq. (2), in which the elastic tensor $\mathbf{D}$ is replaced by the tensor $\frac{\partial \mathbf{D}}{\partial \rho_{m,j}}$. Due to symmetry, $\mathbf{D}$ for two-dimensional problems can be decomposed by

$$\begin{aligned}\mathbf{D} = &\begin{bmatrix} D_{11} & 0 & 0 \\ 0 & 0 & 0 \\ 0 & 0 & 0 \end{bmatrix} + \begin{bmatrix} 0 & D_{12} & 0 \\ D_{12} & 0 & 0 \\ 0 & 0 & 0 \end{bmatrix} + \begin{bmatrix} 0 & 0 & D_{13} \\ 0 & 0 & 0 \\ D_{13} & 0 & 0 \end{bmatrix} \\ &+ \begin{bmatrix} 0 & 0 & 0 \\ 0 & D_{22} & 0 \\ 0 & 0 & 0 \end{bmatrix} + \begin{bmatrix} 0 & 0 & 0 \\ 0 & 0 & D_{23} \\ 0 & D_{23} & 0 \end{bmatrix} + \begin{bmatrix} 0 & 0 & 0 \\ 0 & 0 & 0 \\ 0 & 0 & D_{33} \end{bmatrix}.\end{aligned} \tag{16}$$

The same decomposition applies for $\frac{\partial \mathbf{D}}{\partial \rho_{m,j}}$. Therefore, it is recommended to store each element stiffness matrix (of the macro domain) by 6 parts corresponding to 6 components of $\mathbf{D}$. Once all the element stiffness matrices are evaluated, the derivative of stiffness matrix with respect to micro-scale design variable, $\frac{\partial \mathbf{K}}{\partial \rho_{m,j}}$, can be efficiently calculated.

It is also noticed that in Eq. (12), no sensitivity information of macro densities is required. Hence, sensitivity analysis of micro variables is independent from that of macro variables. In other words, the update of macro densities and the update of micro densities can be done separately. Actually, the sensitivity information is only needed during the update of design variables, e.g. by using the well-known Optimality Criteria (OC) [36, 37]. Therefore, sensitivity analysis of macro densities is not necessary if a gradient-free algorithm is employed for macro-structure.

The authors are aware that currently, multiple micro-structures have been considered. However, the purpose of the current research is to demonstrate the feasibility of introducing gradient-free approach into the two-scale topology optimization. Therefore, we would like to keep the problem as simple as possible. Nevertheless, multiple micro-structures will be included in future works.

2.4. The gradient-free Proportional Topology Optimization (PTO) algorithm

Originally proposed by Biyikli and To [10], the PTO algorithm is an inner loop that distributes material into elements proportionally to the contribution of each element into the objective function (here, the objective is the compliance of the macroscopic structure). The flowchart that describes PTO subroutine can be seen in Ref. [38]. At the start of the inner loop, the target amount of material (TM) is set based on the "mass constraint" (see Eq. (5)). The density value of every element e (of the macro domain) is then distributed by

$$\hat{\rho}_e = RM \frac{c_e}{\sum_{i=1}^{ne} c_i V_i}, \tag{17}$$

in which V_i and c_i and are the area and compliance value of element i, respectively. In order to avoid the well-known checkerboard issue (which is characteristic to density-based topology optimization), a filter is applied as

$$\rho_e = \frac{\sum w_{ej}\hat{\rho}_j}{\sum w_{ej}}, \tag{18}$$

where w_{ej} is the weight value, being evaluated based on the distance between the centers of element e and element j. For more details, please refer to Refs. [10, 12, 38]. RM in Eq. (17) is the remaining material, which is starting as $RM = TM$ and is updated by $RM = RM - \sum \rho_e V_e$. The PTO stops when RM reaches a very small value, e.g. $RM = 0.001\ TM$. After the loop, the density values are determined by

$$\rho_{t+1} = \alpha\rho_t + (1-\alpha)\rho^{PTO}. \tag{19}$$

Here ρ^{PTO} is the density calculated by PTO loop. α plays the role of a coefficient that controls how the densities in the last iteration, ρ_t, and ρ^{PTO} affect the densities in current iteration, ρ_{t+1}. Obviously, $\alpha = 0$ means that history values has no effect, while no update occurs in case $\alpha = 1$.

3. NUMERICAL EXAMPLES

Three benchmark examples are investigated to demonstrate the feasibility of the proposed approach. Without loss of generaility, the material properties are taken as follows: Young's modulus $E = 1$ MPa and Poisson ration $\nu = 0.3$. For finite element mesh, the four-node quadrilateral element is used. In all examples, the unit cell for micro-structure is a square domain of size 0.1×0.1 mm, and is uniformly discretized by 60×60 elements.

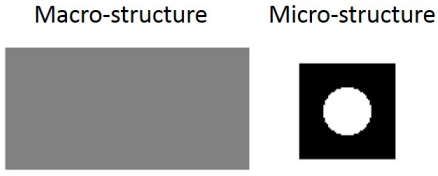

Fig. 2. Illustration of initial designs for macro- and micro-structure. The design domain for macro-structure depends on the example being considered. The design domain for micro-structure in all examples is a square domain of size 0.1×0.1 mm

The initial designs for macro-structure and micro-structure are as follows (see Fig. 2 for illustration):

- Initial design for Macro-structure: the value of every design variable is assigned equally to the volume fraction of macro-structure.

- Initial design for Micro-structure: a circular region at the center of the design domain is left voided, while the design variables outside the voided region are assigned as 1.

In this paper, "the proposed hybrid approach" refers to the employment of gradient-free PTO for macro-scale problem and the gradient-based OC for micro-scale problem. The "complete gradient-based approach" means that OC is used for both scales, which is based on the description in Ref. [20].

The same stopping criteria are used for the Hybrid approach and the Complete gradient-based approach. Commonly in the literatures, it is required that the difference (absolute value) of any arbitrary design variable between the current iteration and the

previous iteration must not exceed a given tolerance (1 % in this paper). The requirement is here applied for both micro- and macro-scale problems.

3.1. Cantilever beam

In this example, the design of a cantilever beam being subject to point load at the middle point of the free end, see Fig. 3, is investigated. A mesh of 60×30 elements is used for the beam.

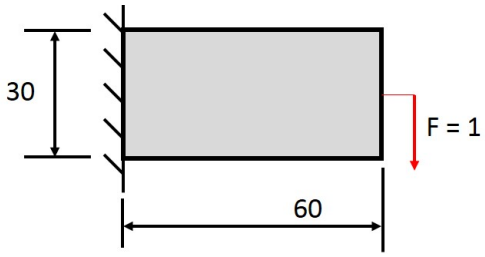

Fig. 3. Schematic sketch of model for design of a cantilever beam

Keeping the volume fraction for the macroscopic beam as 40%, three cases of volume fraction for the microscopic unit cell are considered: a) 40%, b) 60% and c) 100%. As depicted in Fig. 4, the macroscopic designs are quite similar in all three cases, although the compliance value decreases with respect to the increment of micro-structure volume fraction, as reported in Table 1. The micro-structure is symmetric about the x- and y-axes. When volume fraction of micro-structure is 100%, the problem is equivalent to the one-scale problem that considers only the macroscopic structure. Indeed, the two-scale formulation is an extension of the traditional compliance minimization problem, in which

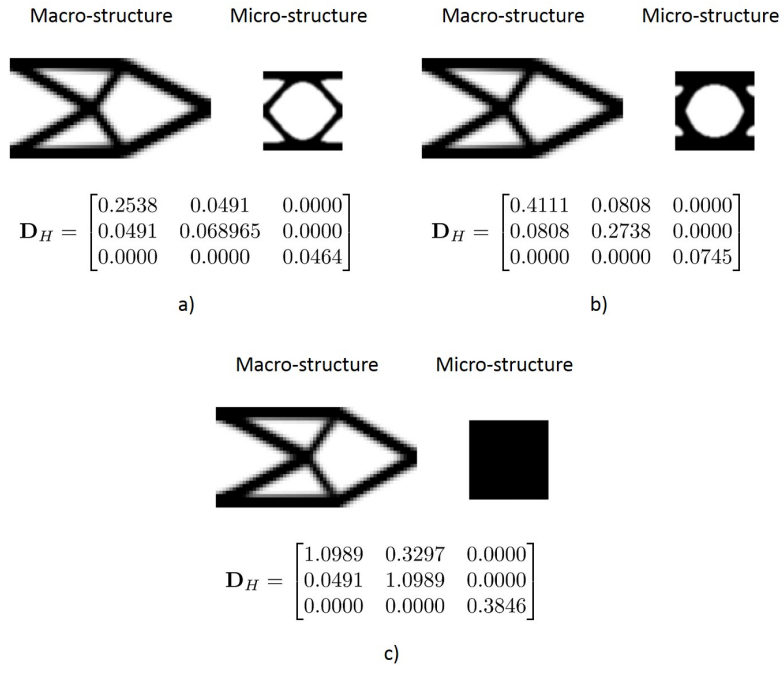

Fig. 4. Topological results obtained by hybrid approach for three values of volume fraction of micro-structure: a) 40%, b) 60% and c) 100%

the design of cellular micro-structures is enabled. Also, it is observed in Table 1 that the hybrid approach is more efficient, in the sense that it gives lower value of compliance and lower elapsed time. The benefit gained is obviously from the utilization of the gradient-free PTO algorithm for the macroscopic problem. The designs obtained by complete gradient-based approach have similar shape with those by the hybrid method and thus, they are not presented for brevity.

Table 1. Comparison on compliance value and elapsed time between the current hybrid and the complete gradient-based approach

Volume fraction of micro-structure		Hybrid	Complete gradient-based
40%	Compliance	507.6708	551.6993
	Iterations	74	115
	Time [s]	~ 718	~ 1316
60%	Compliance	290.0475	314.4254
	Iterations	47	76
	Time [s]	~ 455	~ 784
100%	Compliance	87.9629	95.2080
	Iterations	47	102
	Time [s]	~ 457	~ 1086

It is noted that in Table 1, the advantage of unit square element is not taken into account. When that advantage is exploited, as in Ref. [20], computational time for the problem being considered can be much reduced. However, a mesh of unit square elements is generally not achievable in case of domains with complicated geometry. In other words, the advantage (of unit square element) is no longer applicable in such cases. This issue motivates further research on efficient numerical procedure for problems that involve design domains with general geometrical shapes.

3.2. Curved beam

The problem of a curved beam being subject to a point load, as sketched in Fig. 5 is investigated in this example. For numerical analysis, 2500 four-node quadrilateral elements are used for discretization, see also Fig. 5.

The topological designs for macro- and micro-structures, given that both volume fractions are 40%, are depicted in Fig. 6. It is observed that the micro-structure is not symmetric and thus the homogenized elastic tensor clearly displays anisotropic property. In both cases, complete gradient-based and hybrid approaches, the designs for micro-structure are obtained by the OC algorithm. They are almost identical. However, differences are clearly observed in the macro-structure. The design by the gradient-free PTO algorithm in the hybrid approach has less details but its performance is better (demonstrated by lower value of compliance). Also, the elapsed time by the hybrid approach is smaller.

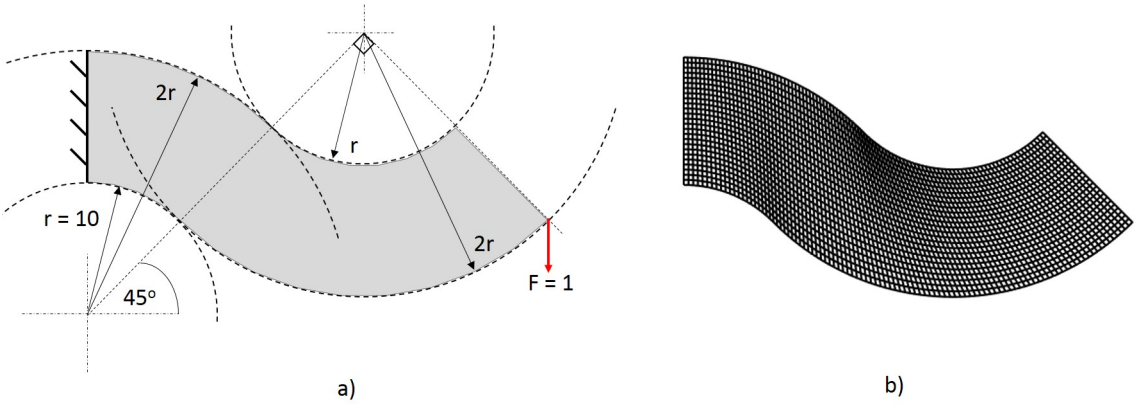

Fig. 5. a) Model, and b) The mesh of 2500 elements of the curved beam being subject to point load

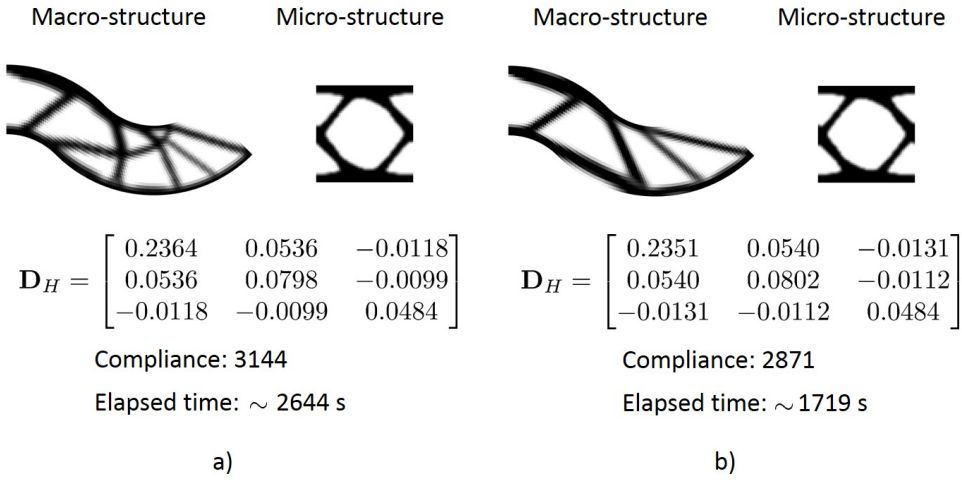

Fig. 6. Topological results for the curved beam obtained by: a) Complete gradient-based approach, and b) Hybrid approach. Volume fraction is 40% for both macro- and micro-scale domains

3.3. Hollow disc being tangentially loaded

The design of a hollow disc being subject to tangential loads is considered in the third example, as shown in Fig. 7. For numerical analysis, a uniform mesh of 6400 four-node quadrilateral elements (40 elements along the radial direction and 1600 elements along the circumferential direction) is employed.

A comparison between the complete gradient-based approach and the proposed hybrid approach is presented in Fig. 8. Again, the performance of hybrid approach is better in terms of computational time and value of objective function. Although the two compliance values are just slightly different, the macroscopic designs are distinctive, especially in the region near the hole.

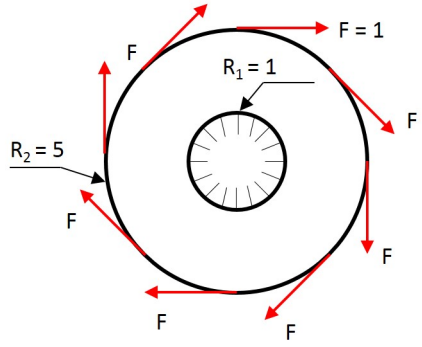

Fig. 7. Model of the hollow disc being tangentially loaded

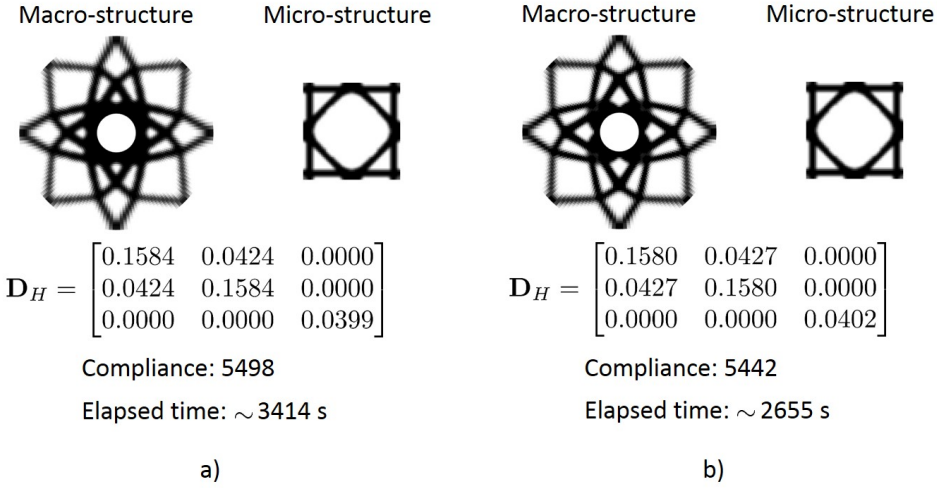

Fig. 8. Topological results for the hollow disc obtained by: a) Complete gradient-based approach, and b) Hybrid approach. Volume fraction is 40% for both macro- and micro-scale domains

4. CONCLUSIONS

The hybrid approach for multi-scale topology optimization of structures is proposed and verified in this paper. The design of macro-structure is conducted by the gradient-free PTO algorithm. For micro-structure, a gradient-free scheme is currently not available. Therefore, the design of micro-structure still relies on the gradient-based OC technique. The sensitivity analysis of each micro-scale design variable requires an evaluation of integral over the macro domain, which is costly. An efficient procedure is thus introduced, which is suitable for domains with complicated geometry (instead of just rectangular domains as in Ref. [20]).

Compared to the procedure that employs OC for both scales, the current hybrid approach generally offers the following advantages:

- Lower computational time;
- Lower value of structural compliance (objective function).

The above efficiency is obviously from the application of PTO in macro-scale problem. This is consistent with the previous works [10, 12, 14].

For each particular problem, the micro-structure may be symmetric or not. Nevertheless, the homogenized elastic tensor is generally not isotropic. This would suggest the necessity to further consider material orientation as design variables [21, 28].

The extension of PTO for the micro-structure is still an open issue. For that purpose, it is necessary to evaluate the contribution of each micro-scale design variable in the objective function. This would be a challenging but interesting topic for future research. Indeed, the current results would facilitate the research on Complete gradient-free approach (using PTO) for the two-scale topology optimization. It can be expected that more benefits could be gained when PTO is employed in both micro- and macro-scale designs. Increasing the computational efficiency when domains with complicated geometries are involved is also an important issue to investigate.

DECLARATION OF COMPETING INTEREST

The authors declare that they have no known competing financial interests or personal relationships that could have appeared to influence the work reported in this paper.

FUNDING

This research received no specific grant from any funding agency in the public, commercial, or not-for-profit sectors.

REFERENCES

[1] M. P. Bendsøe and N. Kikuchi. Generating optimal topologies in structural design using a homogenization method. *Computer Methods in Applied Mechanics and Engineering*, **71**, (2), (1988), pp. 197–224. https://doi.org/10.1016/0045-7825(88)90086-2.

[2] M. P. Bendsøe. Optimal shape design as a material distribution problem. *Structural Optimization*, **1**, (4), (1989), pp. 193–202. https://doi.org/10.1007/bf01650949.

[3] H. P. Mlejnek. Some aspects of the genesis of structures. *Structural Optimization*, **5**, (1-2), (1992), pp. 64–69. https://doi.org/10.1007/bf01744697.

[4] M. Stolpe and K. Svanberg. An alternative interpolation scheme for minimum compliance topology optimization. *Structural and Multidisciplinary Optimization*, **22**, (2), (2001), pp. 116–124. https://doi.org/10.1007/s001580100129.

[5] M. Y. Wang, X. Wang, and D. Guo. A level set method for structural topology optimization. *Computer Methods in Applied Mechanics and Engineering*, **192**, (1-2), (2003), pp. 227–246. https://doi.org/10.1016/s0045-7825(02)00559-5.

[6] S. Kambampati, C. Jauregui, K. Museth, and H. A. Kim. Large-scale level set topology optimization for elasticity and heat conduction. *Structural and Multidisciplinary Optimization*, **61**, (1), (2019), pp. 19–38. https://doi.org/10.1007/s00158-019-02440-2.

[7] A. Takezawa, S. Nishiwaki, and M. Kitamura. Shape and topology optimization based on the phase field method and sensitivity analysis. *Journal of Computational Physics*, **229**, (7), (2010), pp. 2697–2718. https://doi.org/10.1016/j.jcp.2009.12.017.

[8] J. Gao, B. Song, and Z. Mao. Combination of the phase field method and BESO method for topology optimization. *Structural and Multidisciplinary Optimization*, **61**, (1), (2019), pp. 225–237. https://doi.org/10.1007/s00158-019-02355-y.

[9] O. Sigmund. On the usefulness of non-gradient approaches in topology optimization. *Structural and Multidisciplinary Optimization*, **43**, (5), (2011), pp. 589–596. https://doi.org/10.1007/s00158-011-0638-7.

[10] E. Biyikli and A. C. To. Proportional topology optimization: A new non-sensitivity method for solving stress constrained and minimum compliance problems and its implementation in MATLAB. *PLOS ONE*, **10**, (12), (2015). https://doi.org/10.1371/journal.pone.0145041.

[11] M. Cui, H. Chen, J. Zhou, and F. Wang. A meshless method for multi-material topology optimization based on the alternating active-phase algorithm. *Engineering with Computers*, **33**, (4), (2017), pp. 871–884. https://doi.org/10.1007/s00366-017-0503-4.

[12] M. N. Nguyen and T. Q. Bui. Multi-material gradient-free proportional topology optimization analysis for plates with variable thickness. *Structural and Multidisciplinary Optimization*, **65**, (3), (2022). https://doi.org/10.1007/s00158-022-03176-2.

[13] H. Wang, W. Cheng, R. Du, S. Wang, and Y. Wang. Improved proportional topology optimization algorithm for solving minimum compliance problem. *Structural and Multidisciplinary Optimization*, **62**, (2), (2020), pp. 475–493. https://doi.org/10.1007/s00158-020-02504-8.

[14] M. N. Nguyen and T. Q. Bui. A meshfree-based topology optimization approach without calculation of sensitivity. *Vietnam Journal of Mechanics*, **44**, (1), (2022), pp. 45–58. https://doi.org/10.15625/0866-7136/16679.

[15] B. Bochenek and K. Tajs-Zielińska. GOTICA - generation of optimal topologies by irregular cellular automata. *Structural and Multidisciplinary Optimization*, **55**, (6), (2017), pp. 1989–2001. https://doi.org/10.1007/s00158-016-1614-z.

[16] D. Guirguis and M. F. Aly. A derivative-free level-set method for topology optimization. *Finite Elements in Analysis and Design*, **120**, (2016), pp. 41–56. https://doi.org/10.1016/j.finel.2016.06.002.

[17] Y. Luo, J. Xing, and Z. Kang. Topology optimization using material-field series expansion and kriging-based algorithm: An effective non-gradient method. *Computer Methods in Applied Mechanics and Engineering*, **364**, (2020). https://doi.org/10.1016/j.cma.2020.112966.

[18] X. Yan, X. Huang, Y. Zha, and Y. Xie. Concurrent topology optimization of structures and their composite microstructures. *Computers & Structures*, **133**, (2014), pp. 103–110. https://doi.org/10.1016/j.compstruc.2013.12.001.

[19] L. Xia and P. Breitkopf. Concurrent topology optimization design of material and structure within FE^2 nonlinear multiscale analysis framework. *Computer Methods in Applied Mechanics and Engineering*, **278**, (2014), pp. 524–542. https://doi.org/10.1016/j.cma.2014.05.022.

[20] J. Gao, Z. Luo, L. Xia, and L. Gao. Concurrent topology optimization of multiscale composite structures in matlab. *Structural and Multidisciplinary Optimization*, **60**, (6), (2019), pp. 2621–2651. https://doi.org/10.1007/s00158-019-02323-6.

[21] Y. Lu and L. Tong. Concurrent topology optimization of cellular structures and anisotropic materials. *Computers & Structures*, **255**, (2021). https://doi.org/10.1016/j.compstruc.2021.106624.

[22] E. Andreassen and C. S. Andreasen. How to determine composite material properties using numerical homogenization. *Computational Materials Science*, **83**, (2014), pp. 488–495. https://doi.org/10.1016/j.commatsci.2013.09.006.

[23] A. Pizzolato, A. Sharma, K. Maute, A. Sciacovelli, and V. Verda. Multi-scale topology optimization of multi-material structures with controllable geometric complexity — Applications to heat transfer problems. *Computer Methods in Applied Mechanics and Engineering*, **357**, (2019). https://doi.org/10.1016/j.cma.2019.07.021.

[24] M. Al Ali and M. Shimoda. Investigation of concurrent multiscale topology optimization for designing lightweight macrostructure with high thermal conductivity. *International Journal of Thermal Sciences*, **179**, (2022). https://doi.org/10.1016/j.ijthermalsci.2022.107653.

[25] X. Yan, X. Huang, G. Sun, and Y. M. Xie. Two-scale optimal design of structures with thermal insulation materials. *Composite Structures*, **120**, (2015), pp. 358–365. https://doi.org/10.1016/j.compstruct.2014.10.013.

[26] J. Zheng, S. Ding, C. Jiang, and Z. Wang. Concurrent topology optimization for thermoelastic structures with random and interval hybrid uncertainties. *International Journal for Numerical Methods in Engineering*, **123**, (4), (2022), pp. 1078–1097. https://doi.org/10.1002/nme.6889.

[27] A. Ferrer, J. Cante, J. Hernández, and J. Oliver. Two-scale topology optimization in computational material design: An integrated approach. *International Journal for Numerical Methods in Engineering*, **114**, (3), (2018), pp. 232–254. https://doi.org/10.1002/nme.5742.

[28] X. Yan, Q. Xu, H. Hua, D. Huang, and X. Huang. Concurrent topology optimization of structures and orientation of anisotropic materials. *Engineering Optimization*, **52**, (9), (2019), pp. 1598–1611. https://doi.org/10.1080/0305215x.2019.1663186.

[29] P. Liu, Z. Kang, and Y. Luo. Two-scale concurrent topology optimization of lattice structures with connectable microstructures. *Additive Manufacturing*, **36**, (2020). https://doi.org/10.1016/j.addma.2020.101427.

[30] J. Hu, Y. Luo, and S. Liu. Two-scale concurrent topology optimization method of hierarchical structures with self-connected multiple lattice-material domains. *Composite Structures*, **272**, (2021). https://doi.org/10.1016/j.compstruct.2021.114224.

[31] V.-N. Hoang, P. Tran, V.-T. Vu, and H. Nguyen-Xuan. Design of lattice structures with direct multiscale topology optimization. *Composite Structures*, **252**, (2020). https://doi.org/10.1016/j.compstruct.2020.112718.

[32] V.-N. Hoang, P. Tran, N.-L. Nguyen, K. Hackl, and H. Nguyen-Xuan. Adaptive concurrent topology optimization of coated structures with nonperiodic infill for additive manufacturing. *Computer-Aided Design*, **129**, (2020), p. 102918. https://doi.org/10.1016/j.cad.2020.102918.

[33] V.-N. Hoang, N.-L. Nguyen, P. Tran, M. Qian, and H. Nguyen-Xuan. Adaptive concurrent topology optimization of cellular composites for additive manufacturing. *JOM*, **72**, (2020), pp. 2378–2390. https://doi.org/10.1007/s11837-020-04158-9.

[34] L. Xia and P. Breitkopf. Design of materials using topology optimization and energy-based homogenization approach in matlab. *Structural and Multidisciplinary Optimization*, **52**, (6), (2015), pp. 1229–1241. https://doi.org/10.1007/s00158-015-1294-0.

[35] J. Guedes and N. Kikuchi. Preprocessing and postprocessing for materials based on the homogenization method with adaptive finite element methods. *Computer Methods in Applied Mechanics and Engineering*, **83**, (2), (1990), pp. 143–198. https://doi.org/10.1016/0045-7825(90)90148-f.

[36] O. Sigmund. A 99 line topology optimization code written in Matlab. *Structural and Multidisciplinary Optimization*, **21**, (2), (2001), pp. 120–127. https://doi.org/10.1007/s001580050176.

[37] E. Andreassen, A. Clausen, M. Schevenels, B. S. Lazarov, and O. Sigmund. Efficient topology optimization in MATLAB using 88 lines of code. *Structural and Multidisciplinary Optimization*, **43**, (1), (2010), pp. 1–16. https://doi.org/10.1007/s00158-010-0594-7.

[38] M. N. Nguyen, N. T. Nguyen, and M. T. Tran. A non-gradient approach for three dimensional topology optimization. *Vietnam Journal of Science and Technology*, **59**, (3), (2021), pp. 368–379. https://doi.org/10.15625/2525-2518/59/3/14996.